

Primary Effect of SERCA2a Gene Transfer on Conduction Reserve in Chronic Myocardial Infarction

Lukas J. Motloch, MD, PhD;* Marine Cacheux, PhD;* Kiyotake Ishikawa, MD;* Chaoqin Xie, MD; Jun Hu, PhD; Jaume Aguero, MD; Kenneth M. Fish, PhD; Roger J. Hajjar, MD; Fadi G. Akar, PhD, FHRS

Background—SERCA2a gene transfer (GT) improves mechano-electrical function in animal models of nonischemic heart failure. Whether SERCA2a GT reverses pre-established remodeling at an advanced stage of ischemic heart failure is unclear. We sought to uncover the electrophysiological effects of adeno-associated virus serotype 1.SERCA2a GT following myocardial infarction (MI).

Methods and Results—Pigs developed mechanical dysfunction 1 month after anterior MI, at which point they received intracoronary adeno-associated virus serotype 1.SERCA2a (MI+SERCA2a) or saline (MI) and were maintained for 2 months. Age-matched naive pigs served as controls (Control). In vivo ECG-and-hemodynamic properties were assessed before and after dobutamine stress. The electrophysiological substrate was measured using optical action potential (AP) mapping in controls, MI, and MI+SERCA2a preparations. In vivo ECG measurements revealed comparable QT durations between groups. In contrast, prolonged QRS duration and increased frequency of R' waves were present in MI but not MI+SERCA2a pigs relative to controls. SERCA2a GT reduced in vivo arrhythmias in response to dobutamine. Ex vivo preparations from MI but not MI+SERCA2a or control pigs were prone to pacing-induced ventricular tachycardia and fibrillation. Underlying these arrhythmias was pronounced conduction velocity slowing in MI versus MI+SERCA2a at elevated rates leading to ventricular tachycardia and fibrillation. Reduced susceptibility to ventricular tachycardia and fibrillation in MI+SERCA2a pigs was not related to hemodynamic function, contractile reserve, fibrosis, or the expression of Cx43 and Nav1.5. Rather, SERCA2a GT decreased phosphoactive CAMKII-delta levels by >50%, leading to improved excitability at fast rates.

Conclusions—SERCA2a GT increases conduction velocity reserve, likely by preventing CAMKII overactivation. Our findings suggest a primary effect of SERCA2a GT on myocardial excitability, independent of altered mechanical function. (*J Am Heart Assoc.* 2018;7:e009598. DOI: 10.1161/JAHA.118.009598.)

Key Words: arrhythmia • calcium • gene therapy • myocardial infarction

Myocardial infarction (MI) is a primary cause of advanced heart failure (HF) and a major public health epidemic. Patients with post-MI HF exhibit a 5-year mortality rate of >40%. Of note, malignant ventricular tachycardia and fibrillation (VT/VF) account for ≈50% of these deaths.

Unfortunately, conventional therapies for arrhythmias that target sarcolemmal ion channels have often exacerbated rather than improved outcomes in this high-risk patient population,^{1,2} highlighting the need for novel approaches.

One such approach is the use of cardiac gene therapy to restore the expression of calcium (Ca²⁺) cycling proteins, such as the sarco/endoplasmic reticulum Ca²⁺-ATPase 2a (SERCA2a), in an effort to improve mechano-electrical function. Following proof-of-principal studies in rodents, preclinical investigation using adeno-associated virus serotype 1 (AAV1)-mediated SERCA2a gene transfer provided clear benefits in nonischemic HF secondary to either volume overloading in pigs³ or tachycardia pacing in sheep.^{4,5} The utility of this therapy for reversing pre-established cardiac dysfunction when delivered at an advanced stage of ischemic HF caused by chronic MI is unknown, as most studies focused on prevention rather than reversal of cardiac dysfunction. Indeed, this issue is especially important, considering the disappointing outcome of the CUPID 2 (Calcium Upregulation by

From the Cardiovascular Research Center, Icahn School of Medicine at Mount Sinai, New York, NY (L.J.M., M.C., K.I., C.X., J.H., J.A., K.M.F., R.J.H., F.G.A.); Department of Internal Medicine II, Paracelsus Medical University, Salzburg, Austria (L.J.M.).

Accompanying Figures S1 and S2 are available at <https://www.ahajournals.org/doi/suppl/10.1161/JAHA.118.009598>

*Dr Motloch, Dr Cacheux, and Dr Ishikawa contributed equally to this work.

Correspondence to: Fadi G. Akar, PhD, FHRS, Cardiovascular Research Center, Icahn School of Medicine at Mount Sinai, 1470 Madison Ave, 7th floor, Box 1030, New York, NY 10029-6574. E-mail: fadi.akar@mssm.edu
Received April 24, 2018; accepted June 18, 2018.

© 2018 The Authors. Published on behalf of the American Heart Association, Inc., by Wiley. This is an open access article under the terms of the Creative Commons Attribution-NonCommercial License, which permits use, distribution and reproduction in any medium, provided the original work is properly cited and is not used for commercial purposes.

Clinical Perspective

What Is New?

- We demonstrate that SERCA2a gene therapy in pigs following anterior wall myocardial infarction exerts a primary effect on excitability that is fully independent of a change in mechanical function.
- SERCA2a gene therapy increases myocardial conduction reserve, likely by preventing CAMKII activation in this clinically relevant large-animal model of chronic myocardial infarction.

What Are the Clinical Implications?

- Since many conventional therapies for heart failure–related arrhythmias that target sarcolemmal ion channels are fraught with pro-arrhythmic effects, there is a major unmet need for developing novel approaches that are both effective and safe.
- Our findings highlight the safety and potential utility of targeting defective intracellular calcium using a gene therapy approach for improving conduction and ameliorating arrhythmias.

Percutaneous Administration of Gene Therapy in Cardiac Disease Phase 2) trial.⁶

In addition to predisposing to heart failure, MI is a major risk factor for malignant ventricular arrhythmias, which are estimated to account for ≈50% of deaths following MI. A key question is whether accelerating intracellular Ca²⁺ cycling using SERCA2a gene therapy suppresses or promotes post-MI arrhythmias. In rodents, SERCA2a overexpression ameliorated triggered activity by decreasing ryanodine receptor–mediated Ca²⁺ leak.⁷ However, unlike in rodents, post-MI arrhythmias in large animals and humans require an adverse electrophysiological substrate that is capable of converting Ca²⁺-mediated triggers to sustained VT/VF.

The goal of the present study was to investigate the electrophysiological effects of SERCA2a gene therapy when delivered at an advanced stage of ischemic HF caused by chronic MI. The experimental protocol was designed to mimic the clinical scenario of HF treatment by cardiac gene therapy as was the case in CUPID 1 and CUPID 2. We determined the mechanism underlying the electrophysiological effects of SERCA2a gene therapy and their putative relationship to altered mechanical function in this clinically relevant large-animal model of ischemic HF.

Methods

All data, analytic methods, and study materials have been provided within the article.

Animal Protocols

All experimental procedures complied with the National Institutes of Health Guide for the Care and Use of Laboratory

Animals. Protocols were approved by the Institutional Animal Care and Use Committee of the Icahn School of Medicine at Mount Sinai. A detailed time-line of the experimental protocol highlighting the timing of the major procedures is shown in Figure S1. Female Yorkshire pigs were premedicated using intramuscular Telazol (8.0 mg/kg, Fort Dodge, IA). After undergoing placement of an intravenous line, animals were intubated and ventilated with 40% oxygen. General anesthesia was maintained with intravenous propofol (8–10 mg/kg per h) throughout the procedure. Continuous monitoring with an intravenous saline infusion was maintained for a period of 30 minutes to stabilize hemodynamic status. All animals underwent echocardiographic assessment, followed by hemodynamic measurements. All pigs were subjected to extensive anterior MI (procedure described below) and cage-housed for 1 month to develop chronic HF with marked left ventricular (LV) dysfunction compared with control pigs as we have previously reported.⁸ Animal sera were collected at the time of MI to screen for neutralizing antibodies against AAV1.⁹ Only animals with neutralizing antibody titer of <1/2 qualified for AAV1.SERCA2a treatment. Cardiac performance was evaluated at 1 month after MI and pigs received either 3×10¹² vg AAV1.SERCA2a (MI+SERCA2a, N=12) or saline injection (MI, N=14). Two months after the injection, 6-lead ECGs were recorded and cardiac performance was re-evaluated. In a subset of MI (N=8) and MI+SERCA2a (N=8) pigs, dobutamine stress testing was performed for evaluation of contractile reserve and in vivo arrhythmia risk before euthanizing of the animals.

Myocardial Infarction

Boluses of atropine (0.05 mg/kg) and amiodarone (1–3 mg/kg) were administered intravenously or intramuscularly before MI creation. A 1000-mL saline bag mixed with atropine (0.1 mg/kg), amiodarone (3 mg/kg), and potassium acetate (20 mEq) was continuously infused at a rate of 300 mL/h for the duration of the procedure. A 7-Fr hockey-stick catheter (Cordis) was advanced into the left coronary artery. A 0.014-inch guide wire (Abbott, Park, IL) was advanced into the left anterior descending artery and a 4.0-mm VOYAGER over-the-wire balloon (Abbott) was advanced to the proximal end of the coronary artery. The balloon was then inflated to 3 to 4 atm for 120 minutes to interrupt blood flow (Figure S1B) followed by deflation to induce reperfusion. Intramuscular injections of nitroglycerine and furosemide were then administered. Intravenous infusion of saline with amiodarone, atropine, and potassium acetate was adjusted to 50 mL/h and maintained overnight. Animals were returned to their cages and examined daily for signs of pain or distress. Twenty-six pigs that underwent the MI procedure were randomized to receive intracoronary injection of either AAV1.SERCA2a (N=12) or

saline (N=14). The size of the anterior infarct was comparable in MI and MI+SERCA2a pigs (Figure S1C). The control group consisted of pigs (N=15) that did not undergo MI or gene transfer.

AAV1.SERCA2a Construction

AAV1.SERCA2a was produced using the 2-plasmids protocol described by Zolotukhin et al¹⁰ with the following modifications: HEK293T cells (ATCC) were grown in triple flasks for 24 hours (DMEM, 10% fetal bovine serum). Calcium phosphate precipitate was added for cotransfection of plasmid DNA. After 72 hours, the virus was purified from benzonase-treated cell crude lysates over an iodixanol density gradient (Optiprep, Greiner Bio-One Inc), followed by heparin-agarose type I affinity chromatography (Sigma). Finally, the virus was concentrated and formulated into lactated Ringer's solution (Baxter Healthcare Corp) using a Vivaspin 20 Centrifugal concentrators 50K MWCO (Vivascience Inc), and stored at -80°C .

Intracoronary SERCA2a Gene Delivery

A total of 12 pigs underwent SERCA2a gene transfer (MI+SERCA2a) and 14 pigs were given saline injection (MI). Following hemodynamic measurements at the 1-month time-point, nitroglycerin (1 $\mu\text{g}/\text{kg}$ per min) was administered through an intravenous route until the end of the injection procedure. The left coronary artery was cannulated with a 5-Fr hockey stick catheter (CordisVista Brite Tip; Miami, FL). Two 0.014-inch coronary guide wires (Abbott HI-TORQUE ADVANCE, Santa Clara, CA) were introduced into the left anterior descending and left circumflex coronary arteries to fix the position of the catheter.¹¹ A 15-mL bolus of the virus or saline solution diluted 1:1 in blood was infused into the proximal part of the left main coronary artery at 1 mL/min followed by a 5-mL flush of saline/blood mixture at the same flow rate. Similarly, a 5-mL bolus of virus or saline solution mixed 1:1 in blood was infused into the right coronary artery at 1 mL/min followed by a 5-mL flush. We have previously validated the use of this approach in this pig model for restoring SERCA2a expression.¹² As shown in Figure S1D, myocardial SERCA2a expression was significantly higher in AAV1.SERCA2a-treated (MI+SERCA2a) versus untreated (MI) pigs.

In Vivo ECG Analysis

Six-lead ECGs were recorded at the 3-month time-point from control (N=11), MI (N=14), and MI+SERCA2a (N=10) pigs. Baseline (before dobutamine) ECG parameters were measured manually from 7-s ECG epochs by a clinical electrophysiologist who was blinded to the group. QT-interval duration was

corrected for heart rate using the Bazett and Fredericia formulas. An animal was classified as having R' waves if 1 or more ECG leads displayed a secondary R wave consistently throughout the 7-s ECG epoch.

Assessment of Cardiac Performance

A Philips iE-33 ultrasound system (Philips Medical Systems, Andover, MA) was used to acquire echocardiographic data with a multifrequency imaging transducer from MI (N=14) and MI+SERCA2a (N=12) pigs. Complete Doppler transthoracic echocardiographic studies were performed. Images were recorded during end-expiratory breath-hold in the standard LV apical view. Three-dimensional echocardiography data sets were acquired from 4 to 7 consecutive cardiac cycles using the R-wave-triggered mode. An average of 3 data sets were acquired per pig. Postacquisition image analyses were performed using Q-lab (Phillips Medical Systems) by blinded investigators. LV volumes were calculated using 3-dimensional full-volume algorithms including a semi-automated border detection system. The endocardial detection accuracy was manually monitored and optimized. Dobutamine stress (2.5 $\mu\text{g}/\text{kg}$ per min) testing was performed before euthanizing at the terminal 3-month time-point in MI (N=8) and MI+SERCA2a (N=8) pigs. To achieve sufficient loading, pigs were treated with dobutamine for 15 minutes followed by continuous in vivo ECG monitoring (3-lead ECG) for an additional 5 minutes during dobutamine challenge. High-fidelity pressure-volume analysis in response to preload reduction and 3-dimensional echocardiography were performed before and after infusion with dobutamine for 20 minutes. In vivo arrhythmias in response to the dobutamine stress test were assessed by generating an arrhythmia score for each pig as follows: 0: normal sinus rhythm; 1: <5 premature ventricular beats; 2: 5 to 10 premature ventricular beats; 3: 11 to 20 premature ventricular beats; 4: >20 premature ventricular beats or 1 episode of nonsustained VT of ≤ 5 beats; 5: 1 or more episodes of VT lasting >5 beats, or/and multiple episodes of nonsustained VT.

Protein and mRNA Expression Using Western Blot and Quantitative Polymerase Chain Reaction

Frozen tissues from the infarct border of MI (N=6) and MI+SERCA2a (N=5) pigs or a comparable location from noninfarcted control pigs (N=6) were homogenized in RIPA buffer containing protease inhibitor cocktail (Roche) and 20 mmol/L *N*-ethylmaleimide (Sigma-Aldrich) using the MP homogenate system (FastPrep homogenizer). The insoluble portion was removed by centrifugation at 30 000g for 20 minutes. For immunoblotting, cardiac proteins (10–50 μg) were separated by SDS-PAGE, transferred onto a

nitrocellulose membrane (Bio-Rad), and probed with antibodies against GAPDH (Sigma-Aldrich), Nav1.5 (Alomone ASC-005), Cx43 (Sigma C6219), and phosphorylated CAMKII (pierce MA1-047). Blots were developed with Super Signal West Pico (Pierce). Protein band densities were quantified using Image J software (NIH).

Total RNAs from tissue were isolated with RNeasy Isolation kit (Qiagen) and the cDNAs were synthesized from a RT-reaction using High Capacity cDNA Reverse Transcription Kit (Applied Biosystems). Quantitative polymerase chain reactions (PCR) were performed on a real-time PCR system (Applied Biosystems) with SYBR Green PCR Master Mix (Bio-Rad). The following primer sets were used to detect relative gene expression:

Gene Name	Forward Primer (5'–3')	Reverse Primer (5'–3')
GAPDH	CAATGACCCCTTCATTGACC	GAAGATGGTGATGGCCTTTC
CTGF	GTGCACAGCCAAAGATTGTG	TGGTATTTGCAGCTGCTCTG
TGFB	AAAACAGGAAGGCAGTGTGG	TAGGCTGCTTCTTGGCTTC
SMAD3	TTCTCCCTCAACCAAAGTGG	GAGCAGAAGCCATTCTTGC
COL1A1	TTCTGCAACATGGAGACAGG	TCTTGTCTTGGGGTCTTG
COL3A1	TCCTCCTGGAAAGAAATGGTG	TCCAGGCAAGCCTTGTAAATC

In parallel, 1-step reverse transcription PCR (Qiagen) was performed to confirm the specificity of PCR products by gel electrophoresis.

Histology

Formalin-fixed tissue blocks from control, MI, and MI+SERCA2a myocardium were embedded in paraffin, sectioned (7 μ m), mounted, and stained with picro-sirius red for assessing fibrosis. Quantification was performed on 7 control, 7 MI, and 10 MI+SERCA2a pigs (2–6 images per pig).

Optical Action Potential Mapping in Porcine Wedge Preparations

We previously developed the technique of transmural optical action potential (AP) mapping in arterially perfused canine and porcine wedge preparations.^{13–16} This technique has been

extensively used by others in wedges from explanted human hearts.^{17–22} Briefly, wedges of porcine myocardium were dissected from the mid apico-basal region adjacent to the anterior infarct, a region known to support post-MI arrhythmias. Wedges were arterially perfused via a secondary branch of the high lateral or posterolateral left circumflex coronary artery and optical mapping was performed using the voltage-sensitive dye, di-4-ANEPPS.^{13–16,23} Porcine wedge preparations were isolated from control (N=8 pigs, n=11 wedges), MI (N=5 pigs, n=10 wedges), and MI+SERCA2a (N=5 pigs, n=10 wedges) animals. Wedges were paced from the endocardium at a wide range of pacing rates (1.0–5.0 Hz in 0.5-Hz increments) during perfusion with oxygenated (95% O₂, 5% CO₂) Tyrodes solution containing (in mmol/L): NaCl 129, NaHCO₃ 19.9, KCl 4, MgSO₄ 0.41, dextrose 5.5, CaCl₂ 2.5, NaH₂PO₄ 1.0. 1.5 \times the diastolic threshold was used for pacing. Pacing-induced arrhythmias were documented with volume-conducted ECG and optical recordings. Only sustained VT/VF episodes that did not terminate spontaneously were considered in the susceptibility analysis. Pigs with at least 1 inducible preparation that exhibited sustained VT/VF were classified as arrhythmia prone.

Statistical Analysis

N refers to the number of pigs and n to the number of wedges. Hemodynamic measurements and ECG parameters (performed in pigs) are expressed as mean \pm SD. Electrophysiological measurements (performed in wedges) are expressed as mean \pm SEM. Differences between groups were evaluated by χ^2 testing for discrete variables. For continuous variables, the unpaired *t* test was used to compare differences between 2 groups and for multiple-comparisons 1-way ANOVA followed by Tukey test was performed. *P*<0.05 was considered statistically significant.

Results

SERCA2a Gene Therapy Alters In Vivo ECG Parameters in MI Pigs

Before euthanization at the terminal 3-month time-point, in vivo 6-lead ECG parameters were compared in control, MI,

Table 1. In Vivo ECG Analysis

	HR (bpm)	PR (ms)	QRS (ms)	QT (ms)	QT _c [†] (ms)	QT _c [‡] (ms)
Control	90 \pm 17	139 \pm 25	71 \pm 16	380 \pm 50	462 \pm 32	432 \pm 36
MI	76 \pm 13	156 \pm 22	95 \pm 24*	409 \pm 48	459 \pm 40	440 \pm 40
MI+SERCA2a	72 \pm 11	155 \pm 22	78 \pm 21	407 \pm 27	449 \pm 33	435 \pm 26

ECG parameters of evaluated animals obtained 3 months after MI. Data are presented as mean \pm SD. bpm indicates beats per minute; HR, heart rate; MI, myocardial infarction; QT_c[†], corrected QT duration calculated using the Bazett formula; QT_c[‡], corrected QT duration calculated using the Fredericia formula.

**P*<0.05 vs control using ANOVA followed by Tukey's test.

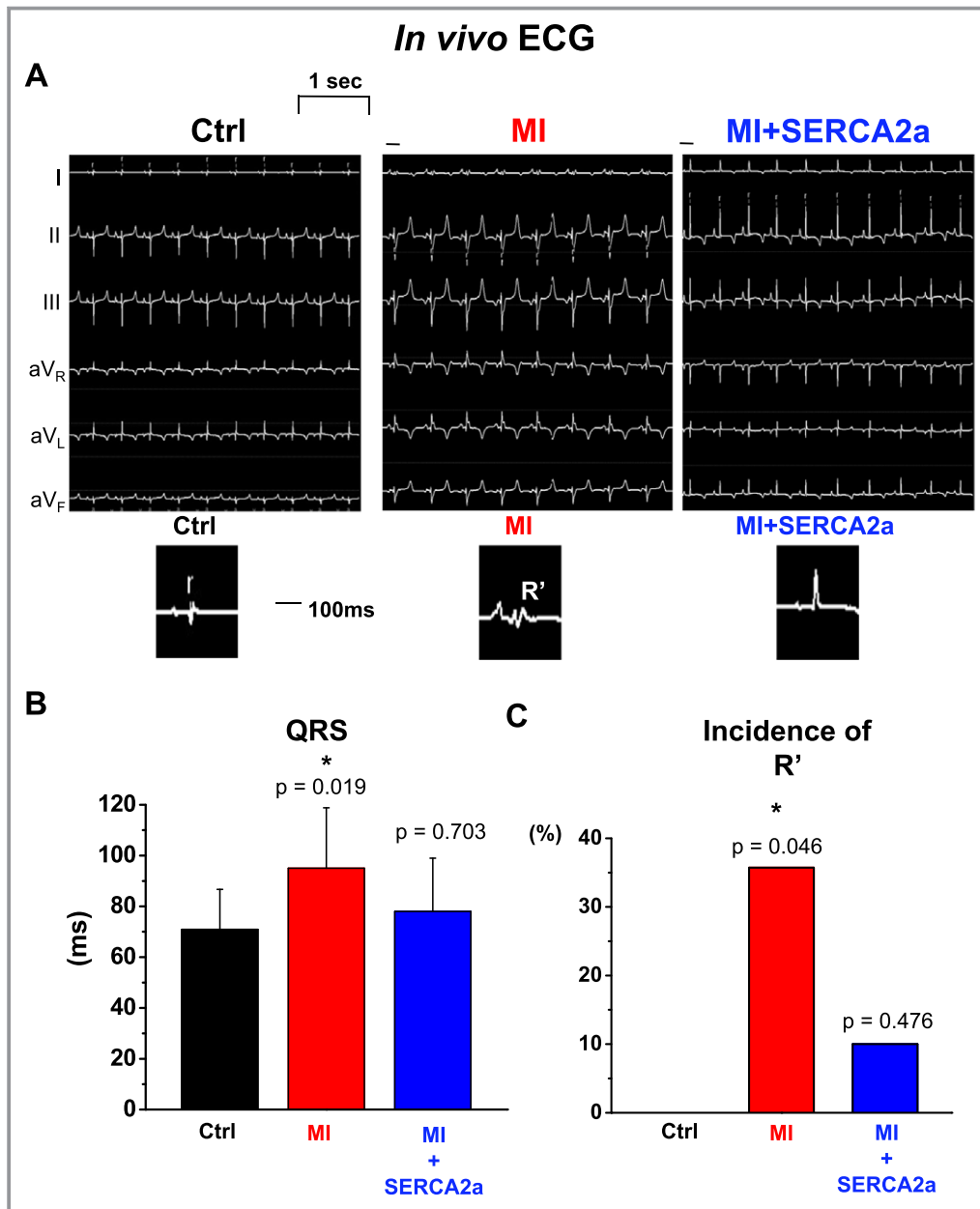


Figure 1. Analysis of 6-lead ECG traces before euthanizing at the 3-month time-point (Ctrl: N=11, MI: N=14, MI+SERCA2a: N=10). A, Representative ECG traces recorded from Ctrl, MI, and MI+SERCA2a animals. B, Compared with Ctrl, MI animals exhibited a significantly wider QRS complex that was ameliorated by SERCA2a gene transfer. C, Percent incidence of R' waves in the 3 groups demonstrating increased incidence in MI and amelioration in MI+SERCA2a relative to Ctrl. * $P < 0.05$ vs Ctrl. Ctrl indicates control; MI, myocardial infarction.

and MI+SERCA2a pigs. As shown in Table 1, PR, QT, QT_c, and average heart rate were similar among groups ($P=NS$). In contrast, MI pigs exhibited a prolonged (by 34%, $P < 0.05$) QRS duration and a tendency towards altered QRS morphology (Figure 1A and 1B). Specifically, we found increased presence of R' waves on the 6-lead ECG recordings in MI pigs (Figure 1C). These ECG changes were unique to the untreated

MI group as they were not present in MI+SERCA2a or control pigs. Further comparison of QRS duration in untreated and SERCA2a-treated MI pigs that exhibited elevated in vivo heart rate (70–100 beats per minute) revealed significantly shorter duration in the latter compared with the former group (Figure 2A). As such, in vivo ECG analysis pointed to a potential role for SERCA2a gene therapy in modifying global

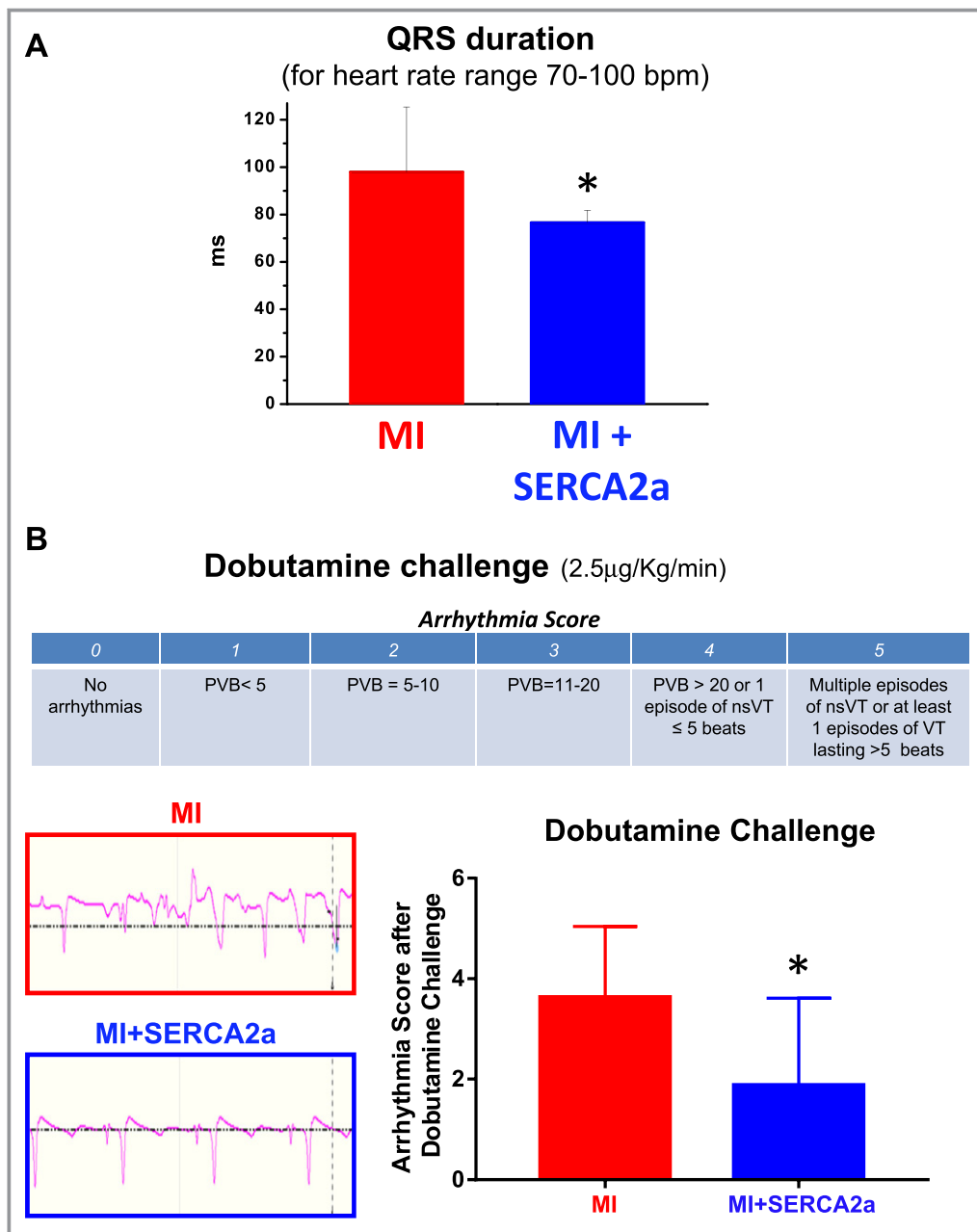


Figure 2. A, In vivo QRS duration in untreated and SERCA2a-treated MI pigs with average heart rate between 70 and 100 bpm (MI: N=10 and MI+SERCA2a: N=6). B, In vivo arrhythmias in response to dobutamine stress testing quantified by a standard arrhythmia score index in MI and MI+SERCA2a pigs (MI: N=8 and MI+SERCA2a: N=8). * $P < 0.05$ vs MI. bpm indicates beats per minute; MI, myocardial infarction; PVB, premature ventricular extra beat; VT, ventricular tachycardia.

cardiac conduction in post-MI pigs. To gain insight into potential differences in susceptibility to arrhythmias, we quantified the arrhythmia score in response to dobutamine stress testing in MI and MI+SERCA2a pigs. As shown in Figure 2B, the arrhythmia score index reflecting the frequency and complexity of in vivo arrhythmic activity was significantly ($P < 0.05$) reduced in MI+SERCA2a compared with untreated MI pigs.

SERCA2a Gene Therapy Alters the Electrophysiological Substrate

Guided by the in vivo ECG findings, we proceeded to investigate the tissue-level electrophysiological substrate using high-resolution optical AP mapping in ex vivo perfused wedge preparations from control, MI, and MI+SERCA2a hearts. Consistent with the QT and QT_c interval durations

measured *in vivo*, we found no significant differences in average action potential duration among control, MI, and MI+SERCA2a preparations (Figure S2A). Moreover, quantification of transmural action potential duration heterogeneity as indexed by the range and SD of action potential duration₈₀ values across the ventricular wall did not reveal significant differences among groups (Figure S1B and S1C).

Instead, we uncovered a major unexpected effect of SERCA2a gene therapy on myocardial conduction, particularly during rapid pacing. Figure 3 shows the rate-dependent adaptation of CV and normalized AP upstroke velocity in control, MI, and MI+SERCA2a preparations. At a basal pacing cycle length of 1000 ms, which approximates the *in vivo* heart rate of pigs, conduction velocity (CV) in untreated and SERCA2a-treated preparations were comparably reduced compared with their control counterparts (Figure 3A). In contrast, differences in average CV between MI and MI+SERCA2a emerged at pacing cycle length of 250 ms (Figure 3A). Analysis of the rate dependence of the normalized upstroke velocity revealed a greater decrease in untreated MI compared with control preparations. Remarkably, SERCA2a gene therapy fully reversed the rate-dependent decrease in this metric of excitability in MI+SERCA2a (Figure 3B).

We therefore surmised that there are intrinsic differences in myocardial conduction reserve between the untreated (MI) and SERCA2a-treated (MI+SERCA2a) groups. Shown in Figure 4A are depolarization isochrone maps recorded from representative MI and MI+SERCA2a preparations that illustrate the crowding of isochrones lines in MI but not MI+SERCA2a preparations as the pacing rate was elevated from 1.0 to 4.0 Hz. On average, when normalized CV (Figure 4B) and AP upstroke velocity (Figure 4C, dF/dt_{max}) were plotted as a function of pacing rate (Hz), a linear relationship was observed with a significantly greater negative slope for MI compared with MI+SERCA2a (Figure 4D and 4E) indicative of greater conduction reserve in the latter compared with the former group at elevated heart rates.

SERCA2a Gene Therapy Suppresses Pacing-Induced Arrhythmias Ex Vivo

Based on our findings of increased myocardial conduction reserve at rapid heart rates in MI+SERCA2a compared with MI hearts, we hypothesized that SERCA2a gene therapy may elicit a protective anti-arrhythmic effect specifically during challenge with rapid pacing. To address this, arterially perfused porcine wedge preparations from control, MI, and MI+SERCA2a pigs were subjected to steady-state pacing at progressively faster rates up to 5.0 Hz or the induction of VT/VF (Figure 5A). Indeed, while none of the control preparations exhibited pacing-induced VT/VF, 80% of MI pigs were

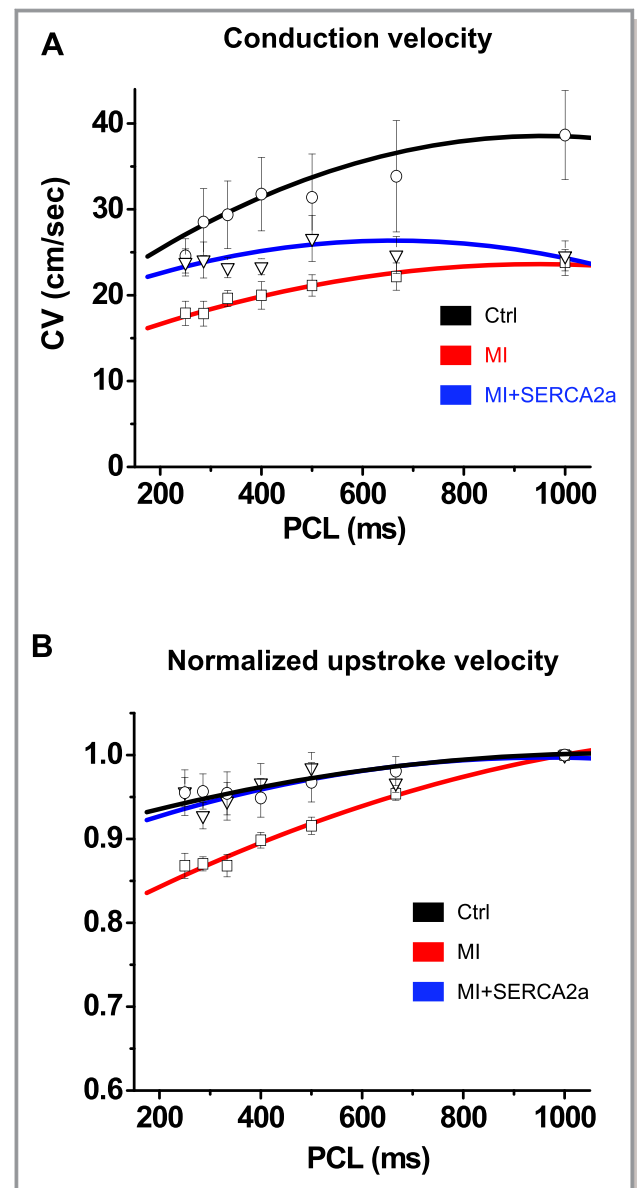


Figure 3. A, PCL-dependent adaptation of CV plotted in Ctrl (n=7 wedges, N=5 pigs), MI (n=8 wedges, N=4 pigs), and MI+SERCA2a (n=8 wedges, N=5 pigs) preparations. B, PCL-dependent adaptation of the normalized AP upstroke velocity relative to that at PCL 1000 ms in preparations from Ctrl (n=7, N=5), MI (n=8, N=4), and MI+SERCA2a (n=8, N=5) animals. AP indicates action potential; CV, conduction velocity; Ctrl, control; MI, myocardial infarction; PCL, pacing cycle length.

susceptible to VT/VF. SERCA2a gene therapy suppressed VT/VF propensity to only 20% of MI+SERCA2a pig hearts (Figure 5B).

Effect of SERCA2a Gene Therapy on Hemodynamic Function

We hypothesized that the beneficial electrophysiological effects of SERCA2a gene therapy may be related to regression

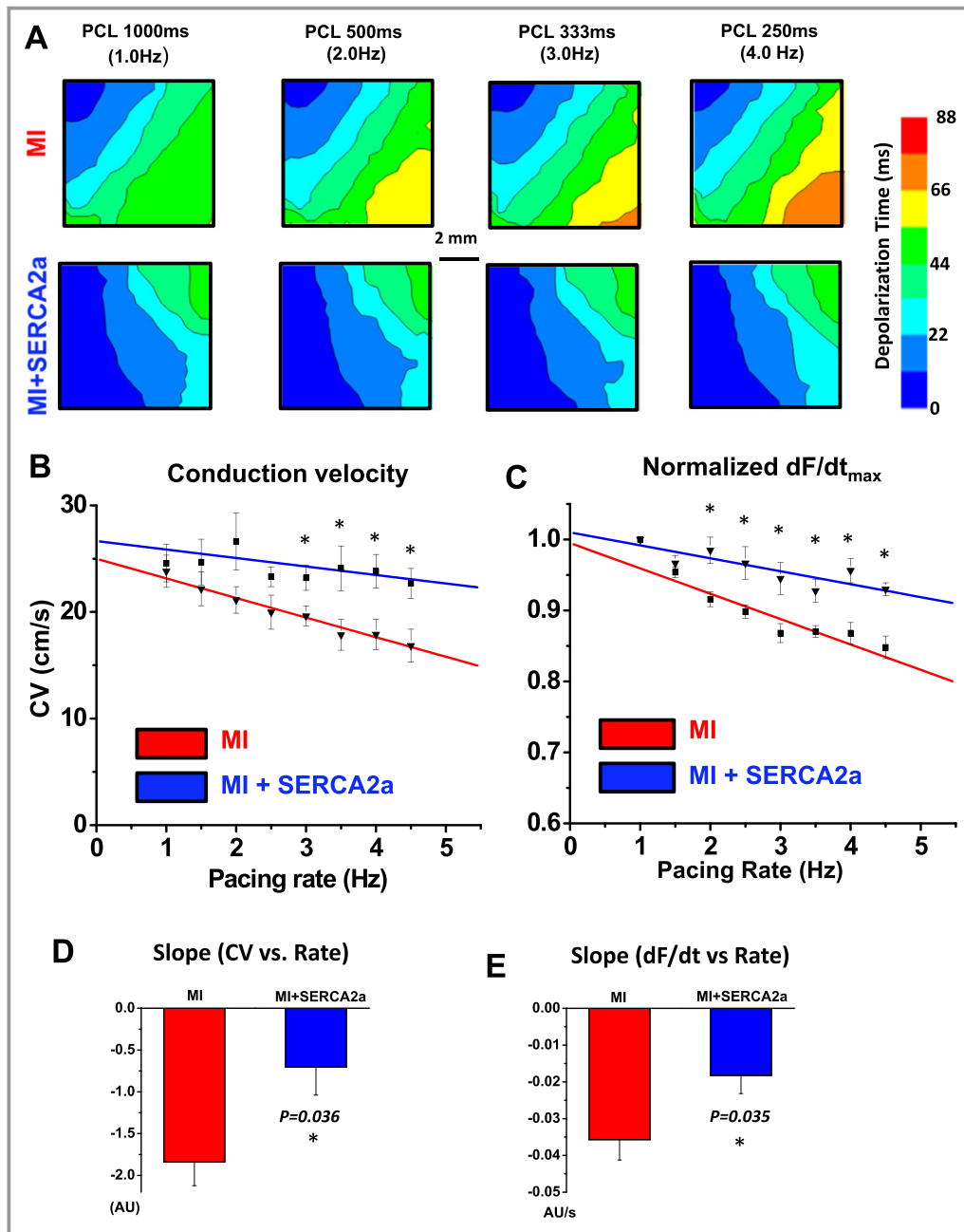


Figure 4. A, Representative depolarization isochrone maps from MI and MI+SERCA2a wedges at PCL 1000, 500, 333, and 250 ms. Conduction velocity in MI (n=8 wedges, N=4 pigs) and MI+SERCA2a (n=8 wedges, N=5 pigs) groups. B, Normalized AP upstroke velocity in MI (n=8 wedges, N=4 pigs), and MI+SERCA2a (n=8 wedges, N=5 pigs). C, Relationship plotted as a function of pacing rate. D, Linear fit of rate-dependent adaptation of CV (left) in wedges from MI and MI+SERCA2a animals demonstrating a significantly steeper slope in MI compared with MI+SERCA2a. E, Linear fit of rate-dependent adaptation of the AP upstroke velocity in wedges from MI and MI+SERCA2a animals. * $P<0.05$ vs MI. AP indicates amplitude; CV indicates conduction velocity; $dF/dt/F$, maximum AP upstroke velocity normalized to the AP amplitude; MI, myocardial infarction; PCL, pacing cycle length.

of HF and improvements in overall mechanical function. We therefore performed a systematic evaluation of hemodynamic properties using invasive pressure-volume analyses and noninvasive echocardiographic measurements. LV volumetric parameters were evaluated by 3-dimensional echocardiography.

Surprisingly, we found no evidence of improved cardiac function either by echocardiography (Table 2) or invasive pressure volume analyses (Table 3). As such, improved electrophysiological parameters were unlikely related to mechanical function. We also tested the response of a

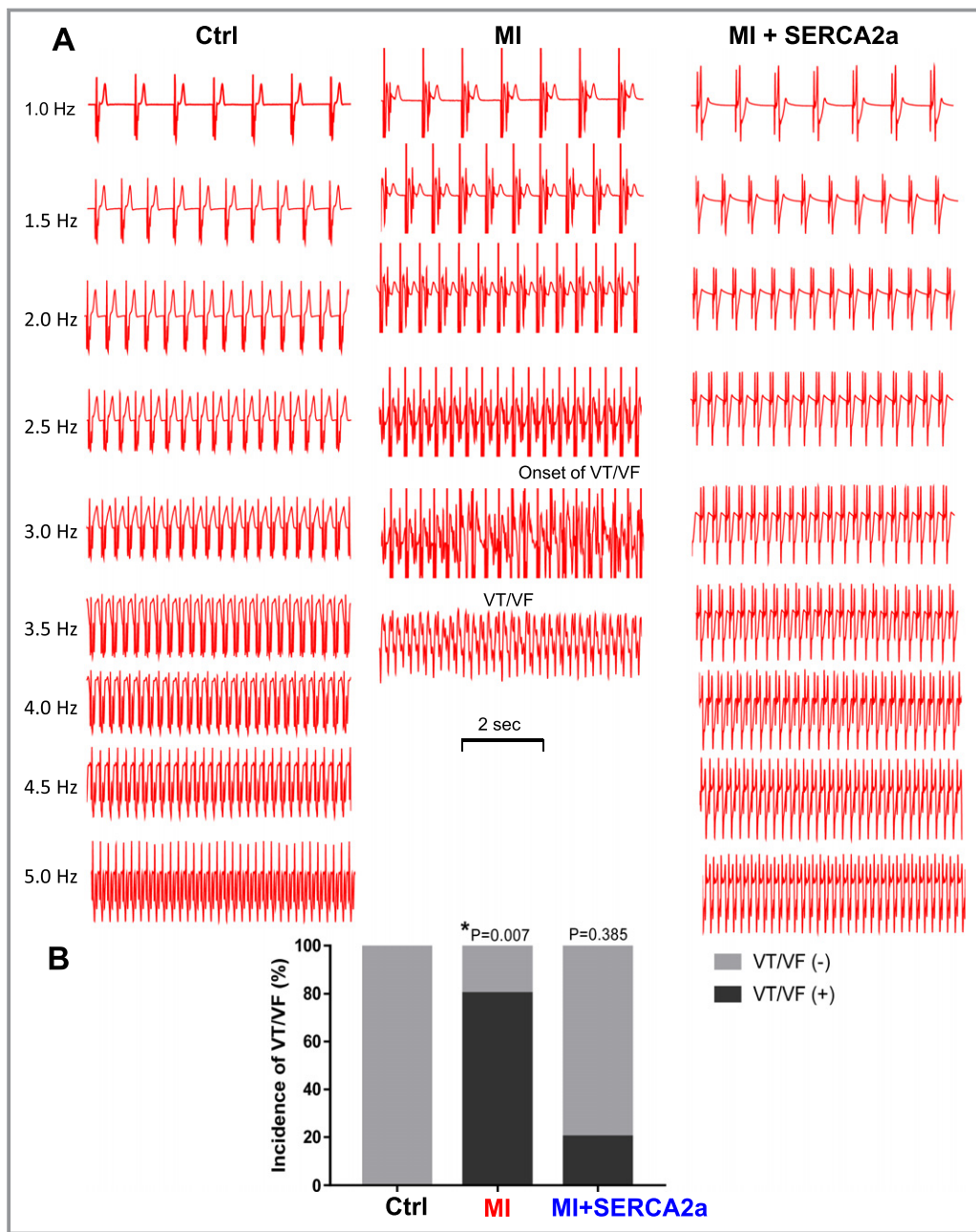


Figure 5. Incidence of VT/VF. A, Representative electrograms recorded in ex vivo perfused preparations from Ctrl, MI, and MI+SERCA2a hearts at progressively increasing pacing rates. Arterially perfused wedges from MI but not MI+SERCA2a or Ctrl animals were prone to VT/VF during challenge with rapid pacing. B, Propensity for VT/VF of Ctrl (N=8), MI (N=5) and MI+SERCA2a (N=5) pigs. A given heart was considered arrhythmia-prone if at least 1 preparation from that heart exhibited pacing-induced VT/VF that was sustained. * $P < 0.05$ vs Ctrl. Ctrl indicates control; MI, myocardial infarction; VT/VF, ventricular tachycardia and fibrillation.

subset of MI and MI+SERCA2a pigs (N=6 per group) to dobutamine (2.5 $\mu\text{g}/\text{kg}$ per minute) challenge as a measure of contractile reserve. As shown in Figure 6, invasive and noninvasive hemodynamic measurements using pressure volume loop analyses and 3-dimensional echocardiography revealed no differences between MI and MI+SERCA2a

pigs before and after dobutamine challenge as end diastolic volume relationship, end systolic pressure volume relationship, preload recruitable stroke work, left ventricular ejection fraction, end diastolic volume, and longitudinal strain were comparable ($P = \text{NS}$ for all indices, Figure 6).

Table 2. Hemodynamic and 3-Dimensional Echocardiographic Parameters

	1 mo			3 mo		
	MI	MI+SERCA2a	P Value	MI	MI+SERCA2a	P Value
Body weight, kg	26.3±4.3	25.3±4.0	0.57	41.5±6.2	42.1±9.6	0.88
P _{max} , mm Hg	88.7±28.1	94.0±13.5	0.55	125.4±16.7	123.4±16.6	0.74
EDP, mm Hg	17.9±3.8	17.2±5.5	0.73	19.2±5.1	15.9±4.6	0.12
dP/dt _{max}	1330±303	1252±362	0.59	2014±632	1796±508	0.37
dP/dt _{min} , mm Hg/s	-1410±379	-1264±512	0.46	-1988±397	-1921±509	0.74
Tau, ms	68.1±17.4	73.7±15.8	0.42	60.3±11.9	61.2±9.4	0.84
HR, bpm	69.2±16.4	71.8±12.4	0.65	76.6±19.1	82.0±15.9	0.46
3D echocardiography						
EF, %	44.2±8.2	43.8±10.2	0.91	44.2±8.7	45.9±8.7	0.63
EDVI, mL/m ²	154.6±39.6	165.2±41.2	0.53	165.7±38.2	169.1±44.9	0.85
ESVI, mL/m ²	88.7±35.5	95.7±37.9	0.65	94.2±33.2	94.7±38.6	0.97
SVI, mL/m ²	65.9±8.4	69.5±12.7	0.45	71.5±12.7	74.4±10.3	0.56

bpm indicates beats per minute; 3D, 3-dimensional; EDP, left ventricular end-diastolic pressure; EDVI, end-diastolic volume index; EF, ejection fraction; ESVI, end-systolic volume index; HR, heart rate; MI, myocardial infarction; P_{max}, left ventricular maximum pressure; SVI, systolic volume index. P value calculated using the unpaired t test with *P<0.05.

Effects of SERCA2a Gene Therapy on the Molecular Determinants of Excitability

Since the favorable impact of SERCA2a gene therapy on myocardial conduction in MI could not be explained by improved hemodynamic status or myocardial contractile reserve assessed by in vivo dobutamine testing, we surmised that there may be a primary effect on the molecular correlates that dictate myocardial conduction. To address this, we examined the expression of the main ventricular gap junction protein Cx43 because of its importance to AP propagation. As shown in Figure 7, total Cx43 expression was decreased by ≈50% in MI compared with control hearts. Despite a trend towards restored expression of total Cx43 by SERCA2a gene therapy, differences between MI and MI+SERCA2a were not statistically significant. We also measured the dephosphorylated (Po) component of

Cx43, which underwent marked upregulation (by >4-fold) in MI compared with control pigs (Figure 7). Increased expression of this dephosphorylated Cx43 component was also not reversed by AAV1.SERCA2a gene therapy (P=0.177 between MI and MI+SERCA2a) (Figure 7).

A hallmark of adverse structural remodeling in ischemic heart disease is the deposition of fibrotic lesions that disrupt myocardial conduction and promote conduction-dependent arrhythmias. We measured the expression of multiple profibrotic markers including connective tissue growth factor (CTGF), transforming growth factor-β (TGF-β), Collagen type 1, alpha 1 (Col1A1), Collagen type 3, alpha 1 (Col3A1), and SMAD3 in MI and MI+SERCA2a hearts relative to control. As shown in Figure 8A, CTGF, TGF-β, and Col1A1 mRNA expression was increased by ≈3-fold (P<0.01) in MI hearts compared with control. Remarkably, SERCA2a gene therapy

Table 3. In Vivo Pressure-Volume Loop Analysis

	1 mo			3 mo		
	MI	MI+SERCA2a	P Value	MI	MI+SERCA2a	P Value
ESPVR						
Slope, mm Hg/mL	1.31±0.32	1.14±0.31	0.21	0.86±0.26	0.77±0.27	0.42
VO, mL	-0.45±17.56	5.43±33.60	0.62	-53.36±37.62	-62.79±83.74	0.75
PRSW						
Slope, mm Hg	32.50±7.71	30.34±11.78	0.62	35.18±9.80	34.59±13.70	0.91
EDPVR						
Slope, mm Hg/mL	0.55±0.17	0.44±0.18	0.14	0.30±0.07	0.25±0.08	0.16

P indicates results of unpaired t test between MI vs MI+SERCA2a. EDPVR indicates end diastolic volume relationship; ESPVR, end systolic pressure volume relationship; MI, myocardial infarction; PRSW, preload recruitable stroke work; VO, volume axis intercept.

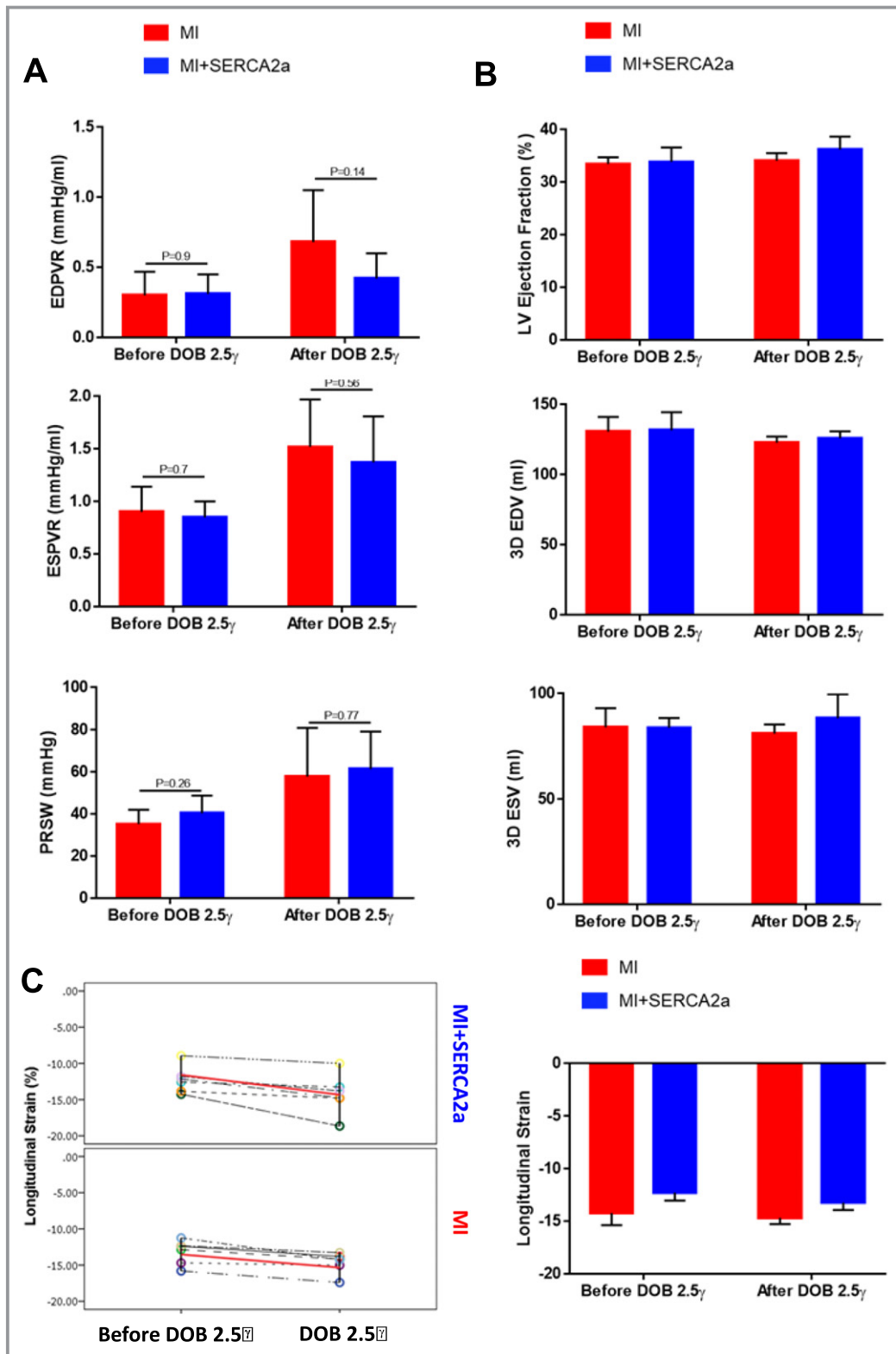


Figure 6. Effects of DOB (2.5 μg/kg per min) treatment. Invasive hemodynamic (A), 3-dimensional echocardiographic (B), and 3-dimensional longitudinal strain (C) measurements in MI (N=6 pigs) and MI+SERCA2a (N=6 pigs) at the terminal time-point before and after DOB stress. DOB indicates dobutamine; EDPVR, end-diastolic pressure volume relationship; EDV, end-diastolic volume; ESPVR, end systolic pressure volume relationship; ESV, end-systolic volume; LV, left ventricular; MI, myocardial infarction; PRSW, preload recruitable stroke work.

fully reversed these changes in profibrosis markers. To determine whether differences in the mRNA expression of profibrotic markers were associated with actual changes in fibrotic content, we determined the extent of fibrosis in histological sections that were stained with picrosirius red (Figure 8B). While samples from untreated MI pigs exhibited a marked rise in picrosirius red staining compared with control, treatment of MI pigs with AAV1-SERCA2a failed to ameliorate this change.

Finally, we found that Nav1.5 expression was comparable across all groups (Figure 9A), discounting a change in the expression of the pore-forming alpha subunit of the sodium channel in the functional changes that we observed. Therefore, we surmised that the differences in the rate dependence of myocardial conduction and excitability are likely related to differences in Na channel activity rather than expression. In recent years, studies have focused on the intricate regulation of Nav1.5 activity by CaMKII,^{24–27} a key calcium-dependent kinase that is activated in MI. In particular, CaMKII activation

was shown to modulate Na channel recovery from inactivation.²⁷ We therefore measured the expression levels of phosphoactive CaMKII (phosphorylated at Thr-287, pCaMKII) levels in control, MI, and MI+SERCA2a hearts. Relative to control, pCaMKII δ protein levels were markedly increased in untreated MI and fully reversed in MI+SERCA2a hearts (Figure 9B).

Discussion

Ventricular tachyarrhythmias account for $\approx 50\%$ of deaths in patients with chronic MI and ischemic HF.²⁸ Since many conventional therapies for HF-related arrhythmias that target sarcolemmal ion channels are fraught with pro-arrhythmic effects, there is a major unmet need for developing novel approaches that are both effective and safe. This is particularly urgent for post-MI patients in whom conventional anti-arrhythmic drugs such as flecainide and sotalol have increased rather than decreased mortality.^{1,2} Because the extent of mechanical dysfunction is a predictor of adverse arrhythmic events, we hypothesized that improving excitation–contraction coupling, mechanical function, and overall heart failure status by restoring SERCA2a expression by gene transfer may improve electrical remodeling and suppress the incidence of malignant arrhythmias.

Despite its success in improving hemodynamic function in animal models, the effective translation of SERCA2a gene therapy to the clinic has faced a major setback as AAV1-SERCA2a gene therapy failed to achieve the preset primary or secondary end points of the CUPID 2 trial. The neutral effects of this therapy in CUPID 2 were likely caused by technical rather than conceptual challenges stemming from inadequate myocardial gene transduction by the chosen gene delivery approach and viral dose. Indeed, very low to absent levels (<10 – 192 ssDNA copy number/ μg human DNA) of transgene DNA were ultimately detected in CUPID 2 patients who underwent left ventricular assist device implantation or cardiac transplantation. As such, failure to achieve robust delivery of the transgene to the myocardium of patients with HF is likely the main culprit for the neutral effects of this clinical trial. The technical limitations that have confounded clinical trials of cardiac gene therapy can be circumvented in animal models in which robust gene delivery can be assured. Therefore, in this study, we were able to address the central question of whether SERCA2a overexpression prevents or provokes arrhythmias in ischemic HF.

To that end, we investigated mechanisms by which SERCA2a gene therapy modulates the electrophysiological substrate and risk of arrhythmias in a clinically relevant pig model of ischemic HF secondary to chronic MI. The major finding is the discovery of an unexpected primary effect of this gene therapy approach on myocardial conduction that is

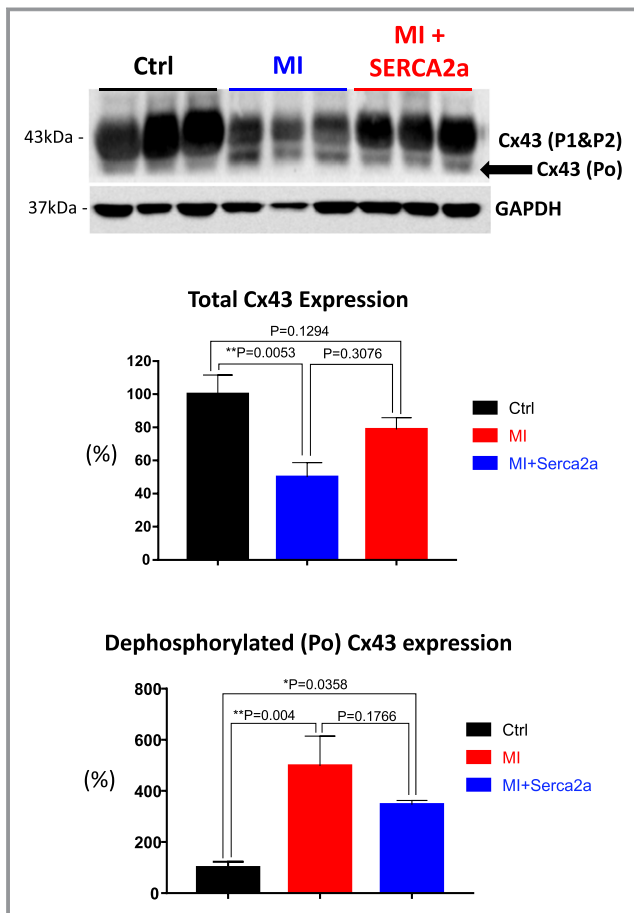


Figure 7. Representative Western blots showing Cx43 expression in Ctrl (N=6), MI (N=6), and MI+SERCA2a (N=5) hearts. Relative total and dephosphorylated (Po) Cx43 expression in MI and MI+SERCA2a compared with Ctrl. Ctrl indicates control; MI, myocardial infarction. * $P < 0.05$; ** $P < 0.01$.

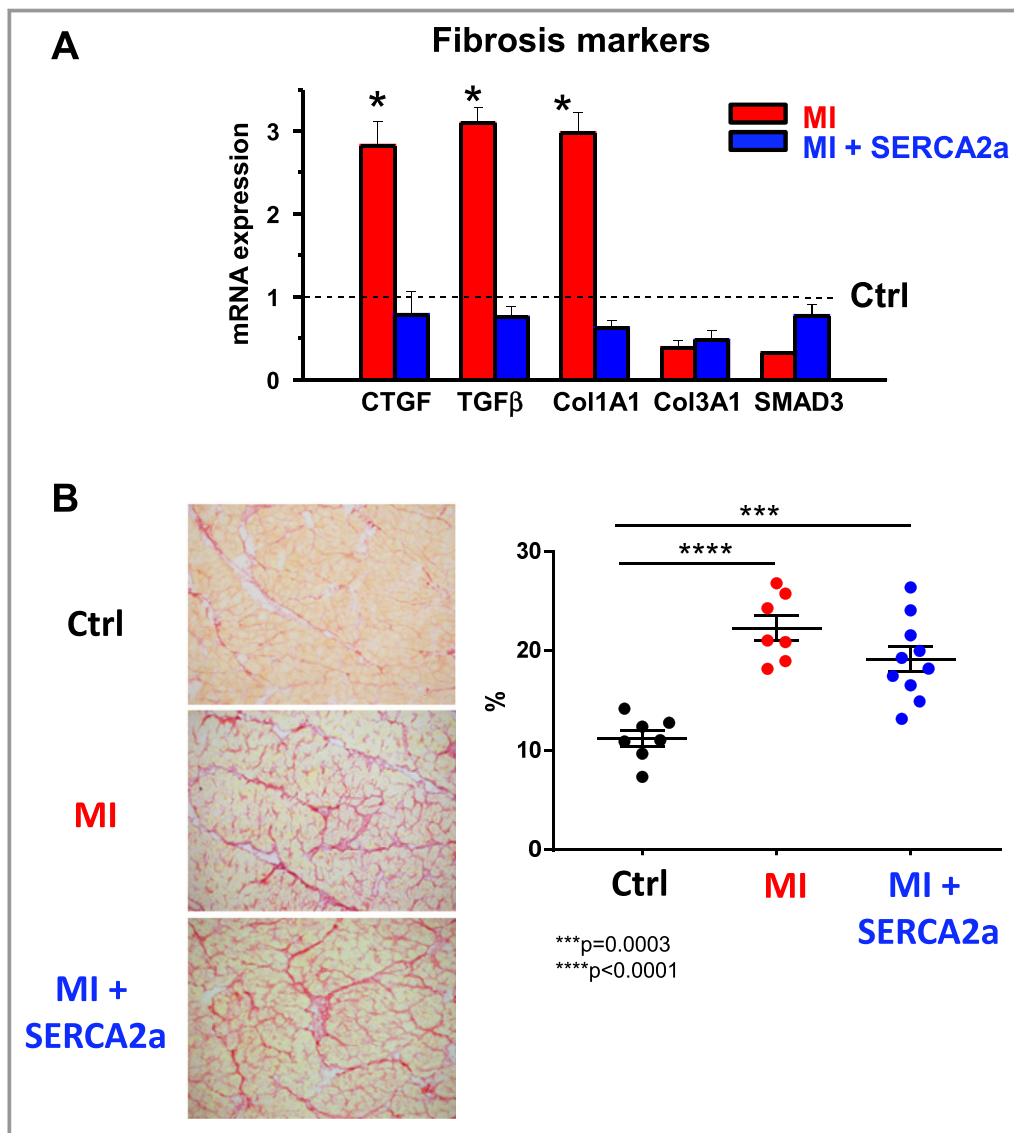


Figure 8. A, Bar graphs show quantitation of mRNA expression of relevant fibrosis markers (CTGF, TGF- β , Col1A1, Col3A1, SMAD3) MI (N=5) and MI+SERCA2a (N=5) hearts normalized to Ctrl (N=5; dotted line). B, Representative images of picrosirius red staining and quantification of the extent of fibrosis in Ctrl, MI, and MI+SERCA2a (Ctrl: N=7, MI: N=7 and MI+SERCA2a: N=10) hearts. Col1A1, Collagen type 1, alpha 1; Col3A1, Collagen type 3, alpha 1; CTGF, connective tissue growth factor; Ctrl, control; MI, myocardial infarction; TGF- β , transforming growth factor- β .

independent of a change in mechanical function. Surprisingly, we found that improved electrophysiological properties by SERCA2a gene therapy could not be explained by differences in hemodynamic function or contractile reserve as assessed by dobutamine testing but rather were caused by direct effects on a molecular target that regulates AP propagation in a rate-dependent manner.

SERCA2a Gene Therapy in Advanced Ischemic HF

The vast majority of previous studies examining the impact of SERCA2a gene therapy on electrophysiological properties in

the failing heart were carried out in rodent models in which arrhythmias depend on calcium-mediated triggered activity. In these earlier studies, SERCA2a gene therapy was effective in suppressing triggered activity by reducing SR calcium leak and spontaneous calcium waves.⁷ Unlike in rodents, however, complex arrhythmias in humans and large animals require an appropriate electrophysiological substrate that converts calcium-mediated triggers into sustained VT/VF. One study in a guinea pig model of pressure overload hypertrophy demonstrated the ability of SERCA2a gene therapy when applied at the time of aortic banding to suppress repolarization alternans.²⁹ However, the impact of SERCA2a gene therapy

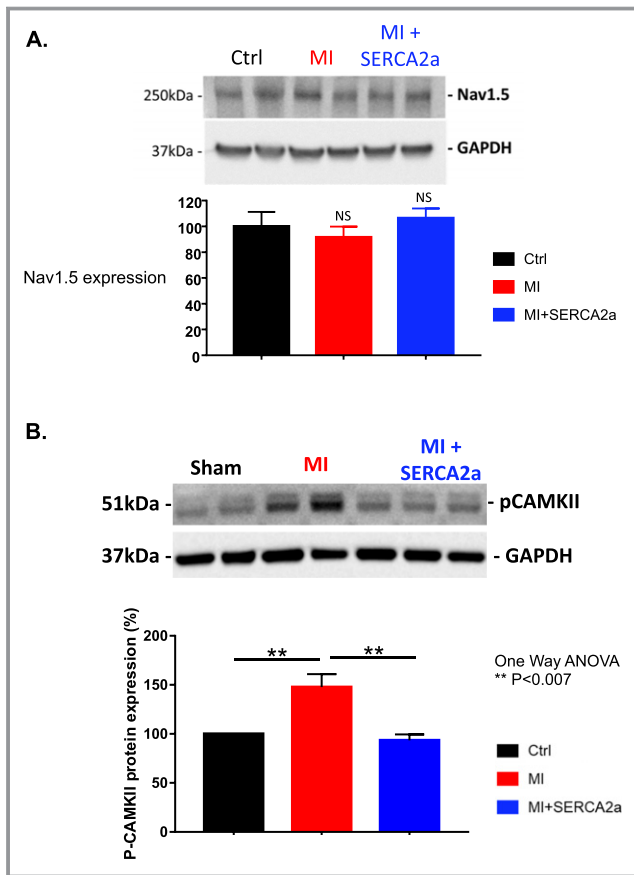


Figure 9. A, Representative Western blots showing Nav1.5 expression in Ctrl (N=3), MI (N=3), and MI+SERCA2a (N=3) hearts (top). Relative Nav1.5 expression in MI and MI+SERCA2a compared with Ctrl. B, Quantification of the active isoform of CaMKII δ phosphorylated at Thr-287 in MI (N=5) and MI+SERCA2a (N=5) relative to Ctrl (N=5). * P <0.05 vs MI. Ctrl indicates control; MI, myocardial infarction; NS, not significant.

on the electrophysiological substrate in clinically relevant large-animal models of ischemic HF remained unknown. A major advantage of our current experimental design was the administration of SERCA2a gene therapy following pre-establishment of LV dysfunction rather than as a preventive measure before its onset. This design was chosen to mimic the clinical scenario of cardiac gene therapy in patients with advanced HF. To our knowledge, this is the first report demonstrating improved myocardial conduction reserve in ischemic HF by a gene therapy approach that targets intracellular calcium cycling.

Effects of SERCA2a Gene Therapy on Myocardial Conduction

Our focus on myocardial conduction was motivated by unexpected in vivo ECG findings in MI and MI+SERCA2a pigs. In particular, we found that SERCA2a gene therapy ameliorates

QRS duration prolongation and suppresses the incidence of R' waves in MI pigs. These changes arose in the absence of any changes in heart rate, PR, or QT intervals implicating SERCA2a gene therapy in the modulation of global ventricular conduction. Consistent with these observations, Katz et al³⁰ demonstrated reversal of QRS prolongation by cardiac surgery-mediated SERCA2a overexpression with recirculation delivery in a sheep model of ischemic heart disease.

Guided by our in vivo ECG findings, we systematically studied the electrophysiological substrate at the tissue level. Indeed, MI+SERCA2a preparations exhibited relatively preserved CV and AP upstroke velocity at fast compared with basal rates. We proceeded to investigate the putative mechanisms and discounted altered expression of Cx43 or Nav1.5 as major factors in the functional changes that we observed. Moreover, while SERCA2a gene therapy reversed the rise in profibrotic gene expression in MI, these changes did not impact actual fibrosis content in histological sections. The lack of impact of our intracoronary gene delivery approach on fibrosis contrasts with the potent fibrosis-suppressing effect of SERCA2a gene delivery by a molecular cardiac surgery approach with recirculating delivery in a sheep model.³¹

Our finding of altered conduction and AP upstroke velocity at fast but not slow rates suggests changes in sodium channel activity rather than expression. CAMKII, a calcium-sensitive kinase that is activated post-MI, regulates Na channel activity in a rate-dependent manner.^{24,25,27} In particular, CAMKII-dependent phosphorylation of Nav1.5 alters I_{Na} gating by reducing current availability at higher pacing rates.²⁷ Moreover, transgenic overexpression of CAMKII δ promotes QRS prolongation and increases predisposition for VT/VF.²⁷ Indeed, phosphoactive CAMKII levels were markedly upregulated in our porcine MI model in agreement with previous results in human and canine models of ischemic heart failure.³² Remarkably, SERCA2a gene therapy in MI pigs reversed the increase in phosphorylated CAMKII levels, likely blunting the rate-dependent reduction in AP upstroke velocity and CV at higher pacing rates. Finally, improved conduction properties at rapid rates in MI+SERCA2a pigs were associated with suppression of arrhythmias. Taken together, our findings support a novel mechanism by which SERCA2a gene therapy can improve electrophysiological function and suppress arrhythmias in chronic MI by increasing myocardial conduction reserve independent of a change in contractile function.

Limitations

Our ex vivo approach for evaluating arrhythmia susceptibility was based on challenge of preparations with fast pacing rates. Indeed, the pacing rates that elicited VT/VF in the wedge preparation do not reflect the typical average heart rates in patients with ischemic HF. Having said that, pacing-induced

arrhythmias in the intact heart are likely to be encountered at much slower rates than those in wedge preparations because of their small dimensions. Moreover, closely coupled premature ventricular beats, which are frequently observed in post-MI hearts, are likely to be associated with similar conduction patterns and arrhythmia risk as shown here for rapid pacing. More importantly, our rapid pacing protocol was chosen to mimic the reported in vivo pig heart rates that are generated in response to vigorous exercise.³³

Conclusion

SERCA2a gene therapy increases myocardial conduction reserve, likely by preventing post-MI CAMKII activation. Our findings suggest a primary effect of SERCA2a gene therapy on myocardial conduction that is independent of mechanical dysfunction.

Sources of Funding

This work was supported by grants from the National Institutes of Health (R01 HL091923 and R21AG054211) and the American Heart Association (13GRNT17000046) to Akar.

Disclosures

None.

References

- Epstein AE, Hallstrom AP, Rogers WJ, Liebson PR, Seals AA, Anderson JL, Cohen JD, Capone RJ, Wyse DG. Mortality following ventricular arrhythmia suppression by encainide, flecainide, and moricizine after myocardial infarction. The original design concept of the cardiac arrhythmia suppression trial (cast). *JAMA*. 1993;270:2451–2455.
- Waldo AL, Camm AJ, deRuyter H, Friedman PL, MacNeil DJ, Pauls JF, Pitt B, Pratt CM, Schwartz PJ, Veltri EP. Effect of D-sotalol on mortality in patients with left ventricular dysfunction after recent and remote myocardial infarction. The SWORD investigators. Survival With Oral D-sotalol. *Lancet*. 1996;348:7–12.
- Kawase Y, Ly HQ, Prunier F, Lebeche D, Shi Y, Jin H, Hadri L, Yoneyama R, Hoshino K, Takewa Y, Sakata S, Peluso R, Zsebo K, Gwathmey JK, Tardif JC, Tanguay JF, Hajjar RJ. Reversal of cardiac dysfunction after long-term expression of SERCA2a by gene transfer in a pre-clinical model of heart failure. *J Am Coll Cardiol*. 2008;51:1112–1119.
- Mariani JA, Smolic A, Prevolos A, Byrne MJ, Power JM, Kaye DM. Augmentation of left ventricular mechanics by recirculation-mediated AAV2/1-SERCA2a gene delivery in experimental heart failure. *Eur J Heart Fail*. 2011;13:247–253.
- Byrne MJ, Power JM, Prevolos A, Mariani JA, Hajjar RJ, Kaye DM. Recirculating cardiac delivery of AAV2/1SERCA2a improves myocardial function in an experimental model of heart failure in large animals. *Gene Ther*. 2008;15:1550–1557.
- Greenberg B, Butler J, Felker GM, Ponikowski P, Voors AA, Desai AS, Barnard D, Bouchard A, Jaski B, Lyon AR, Pogoda JM, Rudy JJ, Zsebo KM. Calcium upregulation by percutaneous administration of gene therapy in patients with cardiac disease (CUPID 2): a randomised, multinational, double-blind, placebo-controlled, phase 2b trial. *Lancet*. 2016;387:1178–1186.
- Lyon AR, Bannister ML, Collins T, Pearce E, Sepehrpour AH, Dubb SS, Garcia E, O'Garra P, Liang L, Kohlbrenner E, Hajjar RJ, Peters NS, Poole-Wilson PA, Macleod KT, Harding SE. SERCA2a gene transfer decreases sarcoplasmic reticulum calcium leak and reduces ventricular arrhythmias in a model of chronic heart failure. *Circ Arrhythm Electrophysiol*. 2011;4:362–372.
- Ishikawa K, Agüero J, Tilemann L, Ladage D, Hammoudi N, Kawase Y, Santos-Gallego CG, Fish K, Levine RA, Hajjar RJ. Characterizing preclinical models of ischemic heart failure: differences between LAD and LCX infarctions. *Am J Physiol Heart Circ Physiol*. 2014;307:H1478–H1486.
- Rapti K, Louis-Jeune V, Kohlbrenner E, Ishikawa K, Ladage D, Zolotukhin S, Hajjar RJ, Weber T. Neutralizing antibodies against AAV serotypes 1, 2, 6, and 9 in sera of commonly used animal models. *Mol Ther*. 2012;20:73–83.
- Zolotukhin S, Byrne BJ, Mason E, Zolotukhin I, Potter M, Chesnut K, Summerford C, Samulski RJ, Muzyczka N. Recombinant adeno-associated virus purification using novel methods improves infectious titer and yield. *Gene Ther*. 1999;6:973–985.
- Ishikawa K, Ladage D, Tilemann L, Fish K, Kawase Y, Hajjar RJ. Gene transfer for ischemic heart failure in a preclinical model. *J Vis Exp*. 2011. Available at: <https://www.jove.com/video/2778/gene-transfer-for-ischemic-heart-failure-in-a-preclinical-model>. Accessed July 31, 2018.
- Tilemann L, Lee A, Ishikawa K, Agüero J, Rapti K, Santos-Gallego C, Kohlbrenner E, Fish KM, Kho C, Hajjar RJ. SUMO-1 gene transfer improves cardiac function in a large-animal model of heart failure. *Sci Transl Med*. 2013;5:211ra159.
- Akar FG, Yan GX, Antzelevitch C, Rosenbaum DS. Unique topographical distribution of M cells underlies reentrant mechanism of torsade de pointes in the long-QT syndrome. *Circulation*. 2002;105:1247–1253.
- Akar FG, Rosenbaum DS. Transmural electrophysiological heterogeneities underlying arrhythmogenesis in heart failure. *Circ Res*. 2003;93:638–645.
- Akar FG, Spragg DD, Tunin RS, Kass DA, Tomaselli GF. Mechanisms underlying conduction slowing and arrhythmogenesis in nonischemic dilated cardiomyopathy. *Circ Res*. 2004;95:717–725.
- Akar FG, Nass RD, Hahn S, Cingolani E, Shah M, Hesketh GG, DiSilvestre D, Tunin RS, Kass DA, Tomaselli GF. Dynamic changes in conduction velocity and gap junction properties during development of pacing-induced heart failure. *Am J Physiol Heart Circ Physiol*. 2007;293:H1223–H1230.
- Boukens BJ, Sulkin MS, Gloschat CR, Ng FS, Vigmond EJ, Efimov IR. Transmural APD gradient synchronizes repolarization in the human left ventricular wall. *Cardiovasc Res*. 2015;108:188–196.
- Glukhov AV, Fedorov VV, Kalish PW, Ravikumar VK, Lou Q, Janks D, Schuessler RB, Moazami N, Efimov IR. Conduction remodeling in human end-stage nonischemic left ventricular cardiomyopathy. *Circulation*. 2012;125:1835–1847.
- Glukhov AV, Fedorov VV, Lou Q, Ravikumar VK, Kalish PW, Schuessler RB, Moazami N, Efimov IR. Transmural dispersion of repolarization in failing and nonfailing human ventricle. *Circ Res*. 2010;106:981–991.
- Holzem KM, Gomez JF, Glukhov AV, Madden EJ, Koppel AC, Ewald GA, Trenor B, Efimov IR. Reduced response to I blockade and altered hERG1a/1b stoichiometry in human heart failure. *J Mol Cell Cardiol*. 2016;96:82–92.
- Lang D, Holzem K, Kang C, Xiao M, Hwang HJ, Ewald GA, Yamada KA, Efimov IR. Arrhythmogenic remodeling of beta2 versus beta1 adrenergic signaling in the human failing heart. *Circ Arrhythm Electrophysiol*. 2015;8:409–419.
- Lou Q, Fedorov VV, Glukhov AV, Moazami N, Fast VG, Efimov IR. Transmural heterogeneity and remodeling of ventricular excitation-contraction coupling in human heart failure. *Circulation*. 2011;123:1881–1890.
- Akar FG, Tomaselli GF. Conduction abnormalities in nonischemic dilated cardiomyopathy: basic mechanisms and arrhythmic consequences. *Trends Cardiovasc Med*. 2005;15:259–264.
- Ashpole NM, Herren AW, Ginsburg KS, Brogan JD, Johnson DE, Cummins TR, Bers DM, Hudmon A. Ca²⁺/calmodulin-dependent protein kinase II (CaMKII) regulates cardiac sodium channel NaV1.5 gating by multiple phosphorylation sites. *J Biol Chem*. 2012;287:19856–19869.
- Hund TJ, Koval OM, Li J, Wright PJ, Qian L, Snyder JS, Gudmundsson H, Kline CF, Davidson NP, Cardona N, Rasband MN, Anderson ME, Mohler PJ. A beta (IV)-spectrin/CaMKII signaling complex is essential for membrane excitability in mice. *J Clin Invest*. 2010;120:3508–3519.
- Koval OM, Snyder JS, Wolf RM, Pavlovicz RE, Glynn P, Curran J, Leymaster ND, Dun W, Wright PJ, Cardona N, Qian L, Mitchell CC, Boyden PA, Binkley PF, Li C, Anderson ME, Mohler PJ, Hund TJ. Ca²⁺/calmodulin-dependent protein kinase II-based regulation of voltage-gated Na⁺ channel in cardiac disease. *Circulation*. 2012;126:2084–2094.
- Wagner S, Dybkova N, Rasenack EC, Jacobshagen C, Fabritz L, Kirchhof P, Maier SK, Zhang T, Hasenfuss G, Brown JH, Bers DM, Maier LS. Ca²⁺/calmodulin-dependent protein kinase II regulates cardiac Na⁺ channels. *J Clin Invest*. 2006;116:3127–3138.
- Greenberg H, Case RB, Moss AJ, Brown MW, Carroll ER, Andrews ML; Investigators M-I. Analysis of mortality events in the Multicenter Automatic

- Defibrillator Implantation Trial (MADIT-II). *J Am Coll Cardiol*. 2004;43:1459–1465.
29. Cutler MJ, Wan X, Plummer BN, Liu H, Deschenes I, Laurita KR, Hajjar RJ, Rosenbaum DS. Targeted sarcoplasmic reticulum Ca²⁺ ATPase 2a gene delivery to restore electrical stability in the failing heart. *Circulation*. 2012;126:2095–2104.
30. Katz MG, Fagnoli AS, Williams RD, Steuerwald NM, Isidro A, Ivanina AV, Sokolova IM, Bridges CR. Safety and efficacy of high-dose adeno-associated virus 9 encoding sarcoplasmic reticulum ca(2+) adenosine triphosphatase delivered by molecular cardiac surgery with recirculating delivery in ovine ischemic cardiomyopathy. *J Thorac Cardiovasc Surg*. 2014;148:1065–1072, 1073e1061–1062; discussion1072–1063.
31. Katz MG, Brandon-Warner E, Fagnoli AS, Williams RD, Kendle AP, Hajjar RJ, Schrum LW, Bridges CR. Mitigation of myocardial fibrosis by molecular cardiac surgery-mediated gene overexpression. *J Thorac Cardiovasc Surg*. 2016;151:1191–1200.e1193.
32. Hund TJ, Decker KF, Kanter E, Mohler PJ, Boyden PA, Schuessler RB, Yamada KA, Rudy Y. Role of activated CaMKII in abnormal calcium homeostasis and I (Na) remodeling after myocardial infarction: insights from mathematical modeling. *J Mol Cell Cardiol*. 2008;45:420–428.
33. D'Allaire S, DeRoth L. Physiological responses to treadmill exercise and ambient temperature in normal and malignant hyperthermia susceptible pigs. *Can J Vet Res*. 1986;50:78–83.

SUPPLEMENTAL MATERIAL

Figure S1. A. Schematic illustration of the study protocol. Myocardial infarction (MI) was created by LAD occlusion *in vivo* followed by reperfusion. **B.** Location of balloon occlusion to induce extensive anterior MI. Coronary balloon was inflated at the proximal LAD just after the take-off of the circumflex artery. Occlusion was maintained for 2 hours followed by reperfusion. **C.** The heart was stained with triphenyl-tetrazolium chloride and the infarcted area was clearly detectable from viable tissue (red). Infarct size was not significantly different between MI (N=14) and MI+SERCA2a (N=12) hearts. **D.** SERCA2a protein expression by western blot analysis in untreated (MI) and AAV1.SERCA2a-treated MI (MI+SERCA2a) pigs. GAPDH was used as a loading control to normalize the data. * P < 0.05 vs Ctrl.

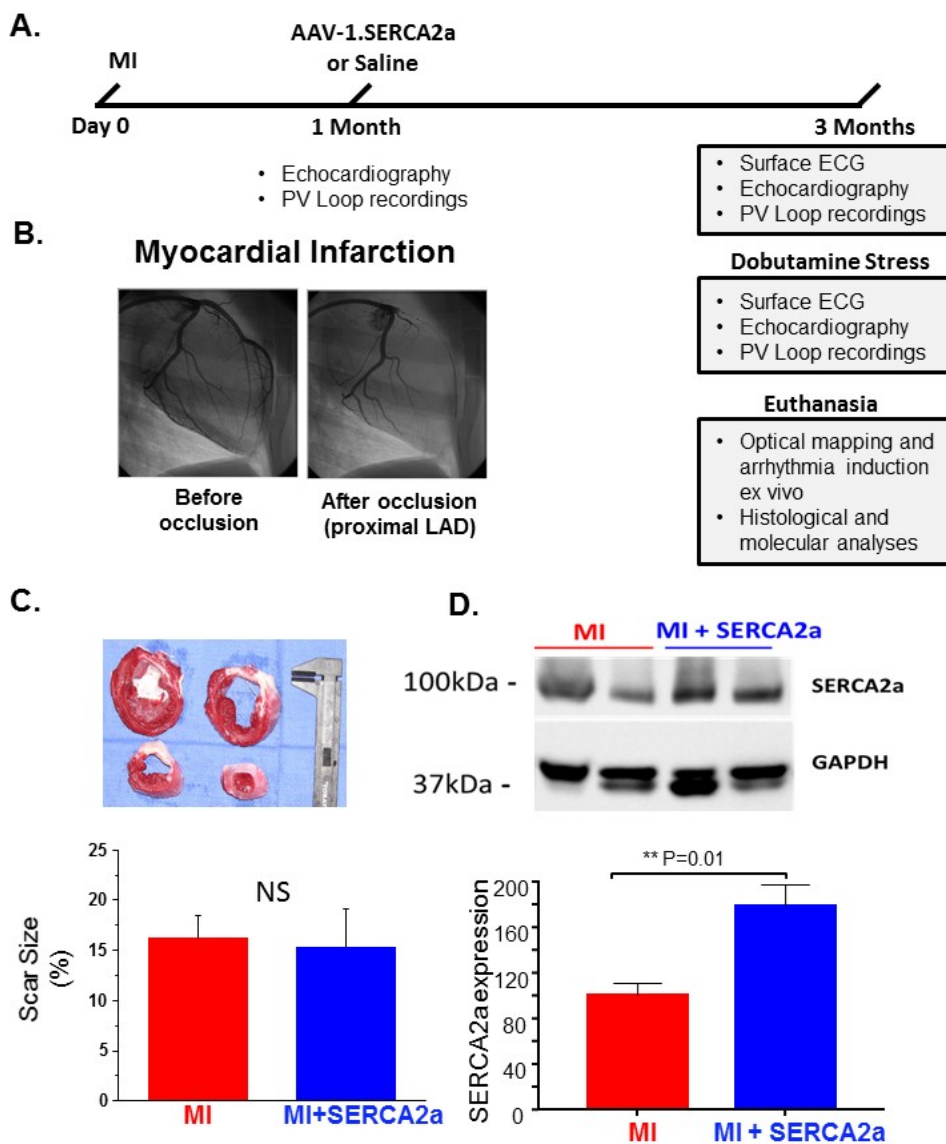


Figure S1

Figure S2. A. Average transmural APD₈₀ values in Ctrl (n=8 wedges, N=5 pigs), MI (n=6, N=3) and MI+SERCA2a (n=8, N=4) measured at basal (PCL 1000ms, left) and rapid rates (PCL 250ms, right). **B&C.** Transmural APD heterogeneity indexed by the standard deviation (SD) and range of APD₈₀ values across the transmural wall at PCL 1000ms (left) and 250ms (right). PCL: pacing cycle length; p-values testing difference between Ctrl, MI and MI+SERCA2a with *p<0.05.

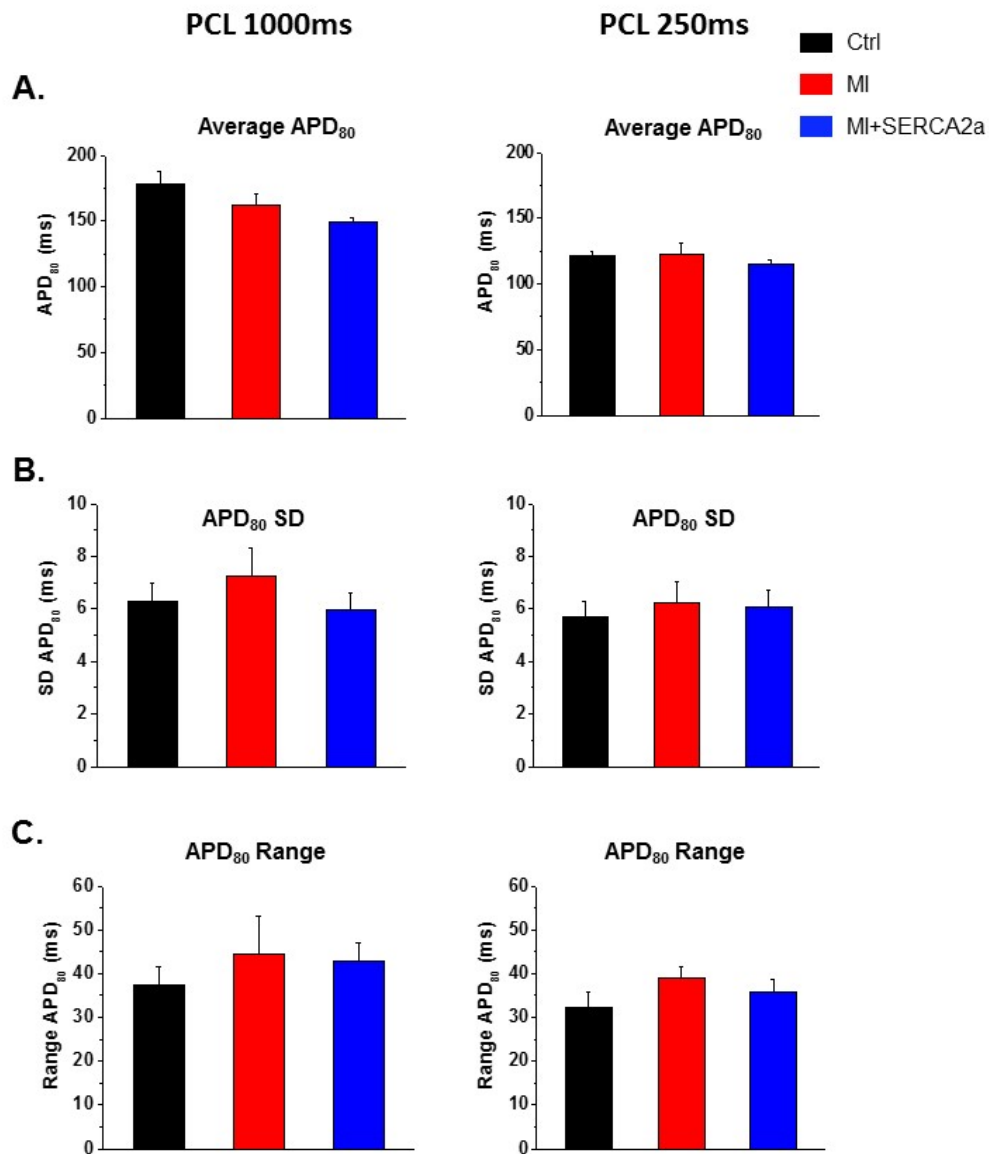


Figure S2